INTERNATIONAL ATOMIC ENERGY AGENCY
UNITED NATIONS EDUCATIONAL, SCIENTIFIC AND CULTURAL ORGANIZATION
INTERNATIONAL CENTRE FOR THEORETICAL PHYSICS
I.C.T.P., P.O. BOX 586, 34100 TRIESTE, ITALY, CABLE: CENTRATOM TRIESTE

SMR.780 - 31

FOURTH AUTUMN COURSE ON MATHEMATICAL ECOLOGY

(24 October - 11 November 1994)

"Seasonality and Extinction in Chaotic Metapopulations"

Bryan Grenfell
Department of Zoology
University of Cambridge
Cambridge CB2 3EJ
United Kingdom

These are preliminary lecture notes, intended only for distribution to participants.

SEASONALITY AND EXTINCTION IN CHAOTIC METAPOPULATIONS

B.T. Grenfell, B.M. Bolker[1] and A. Kleczkowski[2]

Zoology Department
Cambridge University
Downing Street
Cambridge CB2 3EJ
UK

[1] Present address: Department of Ecology and Evolutionary Biology, Princeton University, Princeton, NJ 08544-1003, USA

[2] Present address: Department of Plant Sciences, University of Cambridge, Downing Street, Cambridge CB2 3EA, UK

Key words: Seasonality, extinction, metapopulation, chaos, measles, host, parasite, predator, prey

Short title: Seasonality, chaos and extinction

ABSTRACT

A body of recent work has used coupled logistic maps to show that these model metapopulations show a decrease in global extinction rate in the chaotic region of model behaviour. In fact, many of the main ecological candidates for low dimensional chaos are continuous-time host-parasite and predator-prey systems, driven by strong seasonal 'forcing' of one or more population parameters. This paper therefore explores the relationship between seasonal forcing and metapopulation extinction for such systems. We base the analysis on extensive simulations of a stochastic metapopulation model for measles, based on a standard compartmental model, tracking the density of Susceptible, Exposed, Infectious and Recovered individuals (the SEIR model). The results show that, by contrast with coupled logistic maps, the increased seasonality which causes chaos maintains or increases levels of global extinction of infection, by increasing the synchrony of sub-population epidemics. The model also illustrates that the population interaction (here between susceptible and infective hosts) also has a significant effect on patterns of synchrony and extinction.

INTRODUCTION

A recurrent theme in ecology has been the role of spatial heterogeneity in reducing the extinction rate of populations (Huffaker, 1994; Pimentel *et al.*1963; Hilborn, 1975; Hassell *et al.*1991; Allen *et al.*1993) Recently, Allen et al (1993) and Ruxton (1994) have used coupled logistic maps to derive important theoretical results about the influence of non-linear spatial dynamics on the persistence of metapopulations. They show that increasing the average population reproductive rate (which generates the well known transition from limit cycles to chaos in the logistic map (May, 1976)), decreases local population persistence, while *enhancing* the overall persistence of the metapopulation. Allen et al (who used stochastically perturbed maps) attribute this increase in global persistence to the effect of chaos in amplifying local noise in systems with intermediate coupling. Ruxton (1994) has since shown that this difference in local and global persistence is also generated in the deterministic case - essentially, although there is increased local extinction in the chaotic region, the fluctuations in local populations are sufficiently out of phase to reduce global extinction.

In fact, many of the main ecological candidates for low dimensional chaos are continuous-time host-parasite and predator-prey systems, driven by strong seasonal 'forcing' of one or more population parameters (Hanski *et al.*1993; Aron & Schwartz, 1984; Olsen & Schaffer, 1990; Olsen *et al.*1988). In particular, there is a large literature debating the presence or absence of chaos in measles dynamics in developed countries before the vaccination era (Olsen *et al.*1988; Olsen & Schaffer, 1990; Pool, 1989; Nychka *et al.*1992; Ellner, 1991; Rand & Wilson, 1991; Drepper, 1988). Measles is a particularly good testbed for studies in nonlinear dynamics, because of the availability both of relatively long notification time series (Fine and Clarkson, 1982; Anderson *et al.*1984; Grenfell and Anderson, 1985) and plausible population models (Hamer, 1906; Soper, 1929; Bartlett, 1957; Bartlett, 1960; Black, 1966; Schenzle, 1984; Anderson & May, 1991). Whether or not measles dynamics are chaotic, the effects of seasonality (which arises from the seasonal aggregation of children during school terms) certainly has a strong dynamical impact (Fine & Clarkson, 1982; Schenzle, 1984).

Viewing Allen et al and Ruxton's results in the context of measles dynamics gives rise to two general questions. First, for the forced SEIR model for measles, it is increased *seasonality* which produces chaotic epidemic patterns (Aron & Schwartz, 1984; Olsen & Schaffer, 1990). However, synchronous seasonality might also be expected to magnify the correlation of sub-populations; this might then *increase* metapopulations extinction rates, by synchronising local extinctions. This hypothesis prompts the question: which of these roles of seasonality predominates, in other words, *does increasing seasonality reduce or enhance the extinction rate of model metapopulations?*

The second question concerns the influence of the underlying ecological interaction on the chaos-persistence interaction. In particular, the candidates for seasonally-driven chaos (notably measles and Fennoscandian vole-mustellid cycles - Hanski et al., 1993) reflect the impact of seasonality on functional predator-prey interactions (represented by infectious and susceptible individuals respectively in the case of measles). In this broad class of systems, we therefore address the question: *how does the underlying population interaction affect patterns of extinction?*.

In this paper, we explore these issues using simulations of a model for seasonally forced measles dynamics in a simple host metapopulation. We begin by introducing the structure of the model, then present the results of simulations and finally discuss their ecological implications.

THE MODEL

Model structure

We use a spatial extension of the standard compartmental model for measles - the SEIR model. Though this simple formulation has its shortcomings as a model for many aspects of measles dynamics (Schenzle, 1984; Grenfell, 1992; Bolker & Grenfell, 1993), its well known transition to chaos with increasing seasonal forcing of the infection rate (Aron & Schwartz, 1984; Olsen & Schaffer, 1990) suits our purpose here. Following Allen et al (1993), we divide the constant total host population, of size N_T into 10 equal sub-populations (Nj, j=1, ..., 10). The deterministic dynamics of infection in sub-population j are then described by the following equations.

$$\frac{dS_j}{dt} = \mu N_j - \left(\mu + \beta(t)\left[I_j + \sum_{k \neq j} \nu I_k\right]\right) S_j$$

$$\frac{dE_j}{dt} = \beta(t)\left[I_j + \nu \sum_{k \neq j} I_k\right] S - (\mu + \sigma) E_j \qquad (1)$$

$$\frac{dI}{dt} = \sigma E_j - (\mu + \gamma) I_j$$

S_j, E_j, I_j and R_j respectively represent the density of Susceptible, Exposed, Infectious and Recovered individuals, in a constant local population of size $N_j = S_j + E_j + I_j + R_j$. Average life expectancy, disease incubation, and infectious periods are $1/\mu$, $1/\sigma$, and $1/\gamma$ respectively. The infection rate of susceptibles by infectious individuals is controlled by the parameter $\beta(t)$, which is assumed to be the same for all sub-populations. Seasonality is introduced by making β an annually periodic function of time t: $\beta(t) = b_0(1 + b_1 \cos(2\pi t))$; b_1 measures the amplitude of seasonal variations around the baseline b_0. Finally, cross-infection between sites is controlled by a parameter, v, which can span the range from zero coupling ($v = 0$) to complete homogeneous mixing ($v = 1$).

The simulations

Noise is introduced into the model in two ways. First, we allow for demographic noise by simulating the model with a fully stochastic Monte Carlo procedure (Bartlett, 1957; Olsen *et al.*1988; Olsen & Schaffer, 1990; Bolker & Grenfell, 1993). This approach allows explicitly for the probability of extinction of the infection in the troughs between epidemics. Second, we simulate environmental noise by adding multiplicative Gaussian perturbations to the infection parameters (Rand & Wilson, 1991).

Basic model parameters were adapted from Olsen et al (1988); $b_0 = 0.010107$, $\sigma = 45.6$, $\gamma = 73$, $\mu = 0.02$. Unless otherwise stated, we assume a total population of $N_T = 1$ million hosts, equally divided between the m=10 sub-populations (which therefore each have population size 100,000). This metapopulation size was chosen to give significant global extinction of infection at the minimum level of seasonality used ($b_1 = 0.2$). The above level of b_0 is appropriate for an isolated population of size 100,000; for a given level of coupling (v), b_0 is

scaled down by a factor (1+(m-1)v), to maintain a comparable average force of infection between simulations (Grenfell, 1992). Simulation output was analyzed for 100 years following a 200 year transient. A Poisson immigration rate of 21 infective individuals per year (divided equally across the model metapopulation) was used to reintroduce the infection following global extinction of the infection (Olsen et al., 1988; Grenfell, 1992). Because these simulations are very numerically intensive we only show results for one simulation at each level of seasonality. Further numerical work (replicating a subset of simulations) indicates that the results shown below are representative of model behaviour.

RESULTS

(a) Seasonality and fadeout

Fig. 1 shows patterns of global extinction from simulations at a range of seasonal forcing amplitudes and sub-population couplings. Simulations with demographic noise only and demographic+environmental noise are explored in Figs 1a and b respectively. The figures also display bifurcation diagrams (Allen *et al.*1993), showing the transition of the deterministic SEIR model to chaotic dynamics with increasing seasonality. Overall, these results indicate that there is no tendency for decreased global fade out of infection in the chaotic region of model behaviour. Indeed, if anything, the global extinction rate increases with seasonality, particularly at the higher coupling levels (v=0.01,0.1). Since superimposing environmental noise (Fig 1b) onto the basic demographic variability (Fig. 1a) does not affect this qualitative conclusion, we focus on the demographic case only in the rest of the analysis.

Figure 2 analyses these results in terms of the *correlation structure* of the metapopulation. It shows the relationship between seasonality, chaos and the correlation of sub-population for the case of demographic noise only (corresponding to Fig. 1a). In the simple deterministic, non-spatial, SEIR model, increased seasonal forcing causes period doubling and eventually large amplitude chaos (Figure 1a). However, as shown in Figure 2, increased seasonality in the spatial analogue also causes an increased correlation between sub-populations. Contrary to the result for the logistic map (Allen *et al.*1993; Ruxton, 1994), this increased correlation offsets any tendency for chaos-amplified noise to decrease overall population fade out. We stress that the absence of a negative association between chaotic dynamics and fade out is not specific to measles but is likely to be a generic property of forced predator prey systems.

Fig. 2 also indicates that the slope of the approximately linear relationship between correlation and seasonality increases with the degree of coupling of the metapopulation. Although this effect is partly a function of the slight increase in fadeout with coupling (Fig. 1), it derives mainly from the correlation structure. Specifically, increased coupling raises the lower limit of correlation between sub-populations (which occurs at the lowest level of seasonality - Fig. 2). For a given level of coupling, increased seasonality then magnifies correlation and hence fadeout.

(b) Metapopulation persistence and host-parasite dynamics

(a)Dynamics of extinction Unlike the logistic map models of Allen et al. (1993) and Ruxton (1994), the above results arise from a population interaction, between infective and susceptible hosts. The effects of this (essentially predator-prey) interaction on patterns of metapopulation persistence are explored in Figs 3 and 4. Fig. 3 begins with total susceptible (S) and infective (I) metapopulation trajectories from a section of simulation in the chaotic region (b_1=0.33), which shows significant degrees of fadeout of infection. The time series (Fig. 3a) and associated S vs I phase plot indicate two major epidemics, separated by an infective trough in which the infection repeatedly becomes extinct and is reintroduced by the infective immigration rate. These results clearly illustrate the impact of the underlying population interaction on patterns of metapopulation extinction of infection. First (years 200 and 201) the initial large epidemic depletes the overall density of susceptibles and the infection disappears. Infection is then repeatedly reintroduced by immigration (years 201-202.5). However, although there are minor epidemics, associated with the seasonal increase in infection rate (the latter illustrated by point size in Fig. 3), a major epidemic (year 203) can only occur when susceptible density has been increased sufficiently by births. The equivalent phase portrait (Fig. 3b) , which reflects the characteristic clockwise loop of predator-prey interactions, illustrates this buildup of susceptibles very clearly.

These results for the metapopulation aggregate could, in principle, conceal significant spatial detail in the dynamics. Fig. 4 shows the infective and susceptible time series for individual sub-populations, corresponding with the aggregate results of Fig. 3a and b. Overall, the sub-populations are well correlated - the mean correlation of each with the rest of the aggregate is 0.873, with range 0.43 to 0.96. In other words, most of the susceptible series reflect the decline and subsequent approximately linear increase of the aggregate susceptibles

(Fig. 3a).

Finally, we can explore the timing of epidemics by calculating the critical local threshold density of susceptibles above which a reintroduced infection will become established. From the equilibrium of equations (1), it is routine to show that the effective reproductive ratio of infection is greater than unity - and that a reintroduced infection will therefore spread (Anderson & May, 1991) - above the susceptible threshold.

$$S_j \propto \frac{\gamma}{\beta(t)[1+(m-1)v]} \qquad (2)$$

Fig. 4 displays this threshold; it is periodic, dropping seasonally as infection rates increase. According to simple theory, epidemics are more likely to establish when the local susceptible density is above this limit. Both the sub-population series (Fig. 4) and, in particular, the aggregate data (Fig. 3a) indicate that this is a good approximate criterion for the seasonal sequence of minor epidemics, as well as the synchronous accumulation of susceptibles before the major epidemic in year 203.

(b) Dynamics of metapopulation persistence For comparison with these results, Fig. 3 also shows a time series (Fig. 3c) and phase plot (Fig. 3d) from a section of the same simulation with no fadeouts. The metapopulation dynamics are dramatically different, reflecting an annual pattern of epidemics which is of much lower amplitude than the 3 year cycle of Fig. 3a. The local dynamics (Fig. 5) are even more distinct; the aggregate annual cycles are formed from an irregular and out-of-phase mixture of 1,2 and 3-year epidemics at the local level. This local irregularity is reflected in the generally low correlation of susceptibles in each sub-population with the rest of the aggregate (mean correlation 0.198, range -0.65 to 0.86) - though there is considerable local fadeout, populations are sufficiently out of phase to offset global extinction.

In summary, the details of the population interaction (as well as the pattern of seasonality) have a strong influence on the timing of metapopulation extinction. These results also illustrate that high degrees of fadeout are associated with global synchronisation of local susceptible populations, following large global epidemics.

DISCUSSION

This paper illustrates that the interaction between chaos and metapopulation persistence depends crucially on the origins of the former. By contrast with coupled discrete maps, simple models of seasonally forced predator-prey and host-parasite systems (such as measles) illustrate that strong seasonality tends to maintain or increase metapopulation extinction rates in chaotic systems, by offsetting the ability of chaos to generate local differences in dynamics (Allen *et al.*1993; Ruxton, 1994). As discussed below, periodic windows in model behaviour can enhance infection persistence, however the predominant effect of high seasonality is to maintain gobal extinction rates. This effect occurs over all the levels of population coupling examined. It is also not affected by our implicit assumption that only infected individuals move between sub-populations. Indeed, the coupling effects of seasonality would be magnified if susceptible movement were also allowed. Our results, along with those of Allen et all and Ruxton, stress the potential importance of measuring the *local correlation* of metapopulations when assessing probabilities of extinction.

The second point to emerge from this analysis is that the underlying population interaction also has a significant impact on patterns of persistence. The general point here is that the probability of a successful reintroduction after global extinction depends on the current state of the system. In the context of our model measles metapopulation, this translates to the familiar requirement that there be a sufficient local density of susceptibles for the epidemic to become established (Fig. 4). A corollary of the large epidemics that generate global fadeout of the infection is that the infection dynamics of sub-populations are relatively synchronised (Fig. 4); it is the lack of this synchronisation which prevents extinction (Fig. 5). The latter effect is exactly that postulated by Allen et al (1993) and Ruxton (1994) to explain the reduction in extinctions. Our results show that both periods of persistence and extinction are possible over a wide range of seasonal forcing amplitudes, given the complex intermittent dynamics of the SEIR model (Schwartz, 1985; Bolker & Grenfell, 1993). However, the synchronised major epidemic behaviour, with associated global fadeouts, is maintained or increases with increased seasonality.

As illustrated in Figs 3-5, adding spatial heterogeneity to the forced SEIR model superimposes another level of complexity onto an already intricate dynamical picture. For example, point A in Fig. 1a (the level of fadeout for b_1=0.32, v=0.001) indicates a lower extinction rate of

infection than the points surrounding it (at b_1=0.31,0.33). Extensive simulations of the deterministic model with random starting conditions indicates that the attractor for b_1=0.32 has a propensity for relatively low amplitude (low fadeout) biennial cycles, compared with b_1=0.31 and 0.33.. However, in the spatial stochastic system, this manifests itself as a comparatively high frequency of *annual* metapopulation epidemics, with a significant component of out-of phase biennial patterns in the sub-populations. These results reinforce the point (Sugihara *et al.*1990) that the apparent effect of dynamic nonlinearities can depend crucially on the spatial scale on which they are observed. More work clearly needs to be done to clarify the nonlinear behaviour of forced spatial epidemic models. An important first step here has been made by Schwartz (1992), who analyzed pairs of weakly coupled centres. However, much less work has been done to clarify spatial chaos in more complex forced systems in the presence of noise. We also need to examine further how stochastic effects, and in particular noise-stabilised chaos at relatively low forcing amplitudes (Rand & Wilson, 1991), affect patterns of persistence. However, the present conclusion - that metapopulation extinction rates generally remain high or increase in forced chaotic systems - seems robust.

Ideally, any attempt to model patterns of metapopulation extinction should be related to the persistence of equivalent real systems. Measles, is particularly suitable for this purpose, since relatively long records of incidence are available at a range of spatial scales (Cliff & Haggett, 1988). A major problem with the forced SEIR model is that it appears unable to generate realistic patterns of fade out. The crucial parameter here is the *critical community size*, the average size of urban population to maintain an endemic infection without fade out between major epidemics (Bartlett, 1957; Bartlett, 1960; Black, 1966). This size is observed to be significantly less than a million invididuals (probably around 300-500,000) whereas even spatially disaggregated SEIR models seem unable to persist at populations below several million (Bolker and Grenfell, In preparation).

The problem probably arises because currently models do not correctly represent the impact of spatial and other sources of heterogeneity in measles transmission. For example, one possible spatial refinement is to subdivide our metapopulation more finely. Preliminary analyses indicate that this can reduce the degree of global extinction of infection. However, it also tends to generate unrealistic annual cycles (analogous to those in Fig. 3c,d). Our model also implicitly neglects the effect of distance on mixing of subpopulations. High 'local' mixing

could again act to promote persistence of the infection (Hassell, *et al.*1991). Preliminary work indicates that demographic noise and long range mixing in the stochastic SEIR system tend to destabilise low amplitude, low exrinction patterns arising from local mixing.

Including other heterogeneities, such as a age structure, mitigates these problems of fadeout somewhat (Bolker & Grenfell, 1993). However, fully explaining the dynamics of metapopulation persistence in measles (along with morbilivirus infections of other mammals; (Grenfell *et al.*1992, 1994)) remains a challenge for both epidemiologists and ecologists.

ACKNOWLEDGEMENTS

We thank the following for financial support: Isaac Newton Institute for Mathematical Science (BTG), Royal Society and AFRC (AK) and Mellon Foundation (BMB).

FIGURE LEGENDS

Figure 1 Level of global fadeout (extinction) of infection versus seasonal forcing amplitude for the measles metapopulation simulations described in the text. Fadeout is measured as the proportion of weeks without cases. The figure shows the results for coupling (v) equal to 0.001, 0.01 and 0.1, which probably spans a realistic range for developed-country urban populations (Bolker and Grenfell, in preparation). The corresponding bifurcation diagram for the deterministic attractor is also shown on the figure. At each level of seasonal forcing (b_1), the deterministic system (equations (1)) was simulated for a transient of 1000 years and then the infective density was sampled annually (at the start of each year) for 100 year to generate the points shown. (a) Simulations with demographic noise only. The detailed pattern of fadeout here depends partly on the structure of the attractor at each value of seasonality. For example, for v=0.001 the simulations at point A (b_1=0.32) fade out less than surrounding points. This appears to be partly because, for many starting conditions, the deterministic attractor shows a tendency for regular (low amplitude) biennial cycles at this point in phase space. This point is taken up in the Discussion. (b) Fade-out proportion vs. seasonality for a spatial Monte Carlo model with added noise: all model parameters are as in (a), but now b_0 reflects 'environmental noise' - random changes affecting epidemiological processes - by incorporating 5% Gaussian noise (Rand and Wilson, 1991). At each Monte Carlo step, a new random variate g(t) was picked from a standard normal distribution, and the effective contact rates for that step became ($\beta(t)*(1+0.05*g(t))$).

Figure 2 Cross-correlations vs. fade-out proportion. The figure shows cross-correlations against fade-out proportions (weeks with zero cases) for each of the simulations shown in Figure 1(a). Correlations show overall means of 20-year cross-correlations (Pearson's r) of weekly numbers of infectives in each sub-population. Different symbols show the range of values of cross-coupling (v=0.001,0.01, 0.1). Lines are least squares regressions between fadeout (y) and correlation (x), for each level of coupling. Increased coupling between sub-population increases average correlation (the mean position of the lines) by synchronising large epidemics.

Figure 3 Dynamics of total susceptible and infective density for simulations with demographic noise only (as in Fig. 1a, with b_1=0.33). (a),(b) section of simulation with a period of global

fadeout of infection; (a) and (b) are respectively time and phase space plots for Susceptibles and infectives and the dot size is proportional to the seasonal swing of infections rate ($\beta(t)$). (c),(d) - as (a),(b), but for a region of the simulation with no fadeouts.

Figure 4 Time plots of susceptible (bold dots) and infective (dashed line) densities for 4 of the 10 sub-populations, corresponding to Fig. 3a. The periodic dotted curve is the critical local density of susceptibles for establishment of the infection, calculated from equation (2).

Figure 5 As Fig. 4, but for the simulation of Fig. 3c.

REFERENCES

Allen, J.C., Schaffer, W.M. & Rosko, D. 1993 Chaos reduces species extinction by amplifying local population noise. *Nature*. **364**, 229-232.

Anderson, R.M., Grenfell, B.T. & May, R.M. 1984 Oscillatory fluctuations in the incidence of infectious disease and the impact of vaccination: time series analysis. *J. Hyg. (Camb.)*. **93**, 587-608.

Anderson, R.M. & May, R.M. 1991 *Infectious diseases of humans: dynamics and control.* Oxford University Press.

Aron, J.L. & Schwartz, I.B. 1984 Seasonality and period-doubling bifurcations in an epidemic model. *J. Theor. Biol.* **110**, 665-679.

Bartlett, M.S. 1957 Measles periodicity and community size. *J. Roy. Stat. Soc. A* **120**, 48-70.

Bartlett, M.S. 1960 The critical community size for measles in the U.S. *J. Roy. Stat. Soc. A* **123**, 37-44.

Black, F.L. 1966 Measles endemicity in insular populations: critical community size and its evolutionary implication. *J. Theor. Biol.* **11**, 207-211.

Bolker, B.M. & Grenfell, B.T. 1993 Chaos and biological complexity in measles dynamics. *Proc. R. Soc. Lond. Biol.* **251**, 75-81.

Cliff, A.D. & Haggett, P. 1988 *Atlas of Disease Distributions: Analytic Approaches to Epidemiologic Data*. Oxford: Basil Blackwell.

Drepper, F.R. 1988 Unstable determinism in the information production profile of an epidemiological time series. In *Ecodynamics: contributions to theoretical ecology*. (ed. W. Wolff, C.-J. Soeder & F.R. Drepper), pp. 319-332. London: Springer-Verlag.

Ellner, S. 1991 Detecting low-dimensional chaos in population dynamics data: a critical review. In *Does Chaos Exist in Ecological Systems?* (ed. J. Logan & F. Hain), University Press of Virginia.

Fine, P.E.M. & Clarkson, J.A. 1982 Measles in England and Wales-I: an analysis of factors underlying seasonal patterns. *Int. J.* Epidem. **11**, 5-15.

Grenfell, B.T. 1992 Chance and chaos in measles dynamics. *J. Roy. Stat. Soc. B.* **54**, 383-398.

Grenfell, B.T. and Anderson, R.M. (1985). The estimation of age-related rates of infection from case notifications and serological data. *J. Hyg.(Camb.)* **95**, 419-436.

Grenfell, B.T., Lonergan, M.E. & Harwood, J. 1992 Quantitative investigations of the epidemiology of phocine distemper virus (PDV) in European common seal populations. *Sci. Tot. Env.* **115**, 15-28.

Grenfell, B.T., Kleczkowski, A., Ellner, S. and Bolker, B.M. (1994). Measles as a case study in nonlinear forecasting and chaos. *Phil. Trans. R. Soc. Lond. Biol.* (In press).

Hamer, W.H. 1906 Epidemic disease in England-the evidence of variability and of persistency of type. *Lancet.* **1**, 733-739.

Hanski, I., Turchin, P., Korpimaki, E. & Henttonen, H. 1993 Population oscillations of boreal rodents: regulation by mustelid predators leads to chaos. *Nature.* **364**, 232-235.

Hassell, M.P., Comins, H.N. & May, R.M. 1991 Spatial structure and chaos in insect population dynamics. *Nature.* **353**, 255-258.

Hilborn, R. 1975 The effect of spatial heterogeneity on the persistence of predator-prey interactions. *J. Theor. Biol.* **8**, 346-355.

Huffaker, C.B. 1994 Experimental studies on predation: dispersion factors and predator-prey interactions. *Hilgardia.* **27**, 343-383.

May, R.M. 1976 Simple mathematical models with very complicated dynamics. *Nature*. **261**, 459-467.

Nychka, D., Ellner, S., Gallant, A.R. & McCaffrey, D. 1992 Finding chaos in noisy systems. *J. Roy. Stat. Soc. B*. **54**, 399-426.

Olsen, L.F., Truty, G.L. & Schaffer, W.M. 1988 Oscillations and chaos in epidemics: a nonlinear dynamic study of six childhood diseases in Copenhagen, Denmark. *Theor. Popul. Biol.* **33**, 344-370.

Olsen, L.F. & Schaffer, W.M. 1990 Chaos versus noisy periodicity: alternative hypotheses for childhood epidemics. *Science*. **249**, 499-504.

Pimentel, D., Nagel, W.P. & Madden, J.L. 1963 Space-time structure of the environment and the survival of parasite-host systems. *Am. Nat.* **97**, 141-167.

Pool, R. 1989 Is it chaos, or is it just noise? 1. *Science*. **243**, 25-28.

Rand, D.A. & Wilson, H. 1991 Chaotic stochasticity: a ubiquitous source of unpredictability in epidemics. *Proc. R. Soc. Lond. Biol.* **246**, 179-184.

Ruxton, G.D. 1994 Low levels of immigration between chaotic populations can reduce system extinctions by inducing asynchronous regular cycles. *Proc. R. Soc. Lond. Biol.* (In press)

Schenzle, D. 1984 An age-structured model of pre- and post-vaccination measles transmission. *IMA. J. Math. Appl. Med. Biol.* **1**, 169-191.

Schwartz, I.B. 1985 Multiple recurrent outbreaks and predictability in seasonally forced nonlinear epidemic models. *J. Math. Biol.* **21**, 347-361.

Schwartz, I.B. 1992 Small amplitude, long period outbreaks in seasonally driven epidemics. *J. Math. Biol.* **30**, 473-491.

Soper, M.A. 1929 The interpretation of periodicity in disease prevalence. *J. Roy. Stat. Soc. A* **92**, 34-61.

Sugihara, G., Grenfell, B.T. and May, R.M. (1990). Distinguishing error from chaos in ecological time series. *Phil. Trans. R. Soc. Lond. Biol.* 330, 235-251.

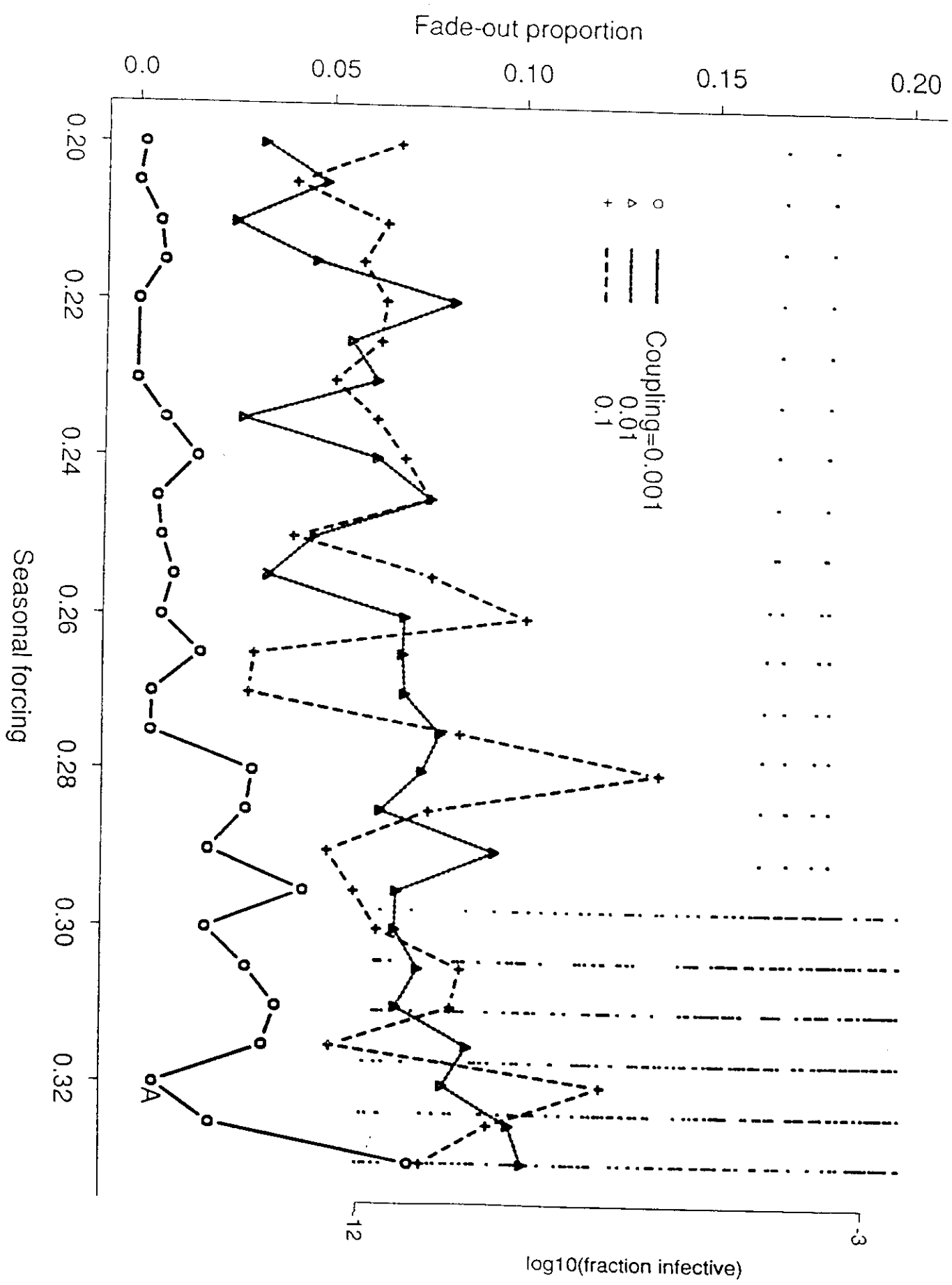
Fade-out proportion
0.0
0.05
0.10
0.15
0.20
Seasonal forcing
0.20
0.22
0.24
0.26
0.28
0.30
0.32
A
Coupling=0.001
0.01
0.1
-12
-3
log10(fraction infective)

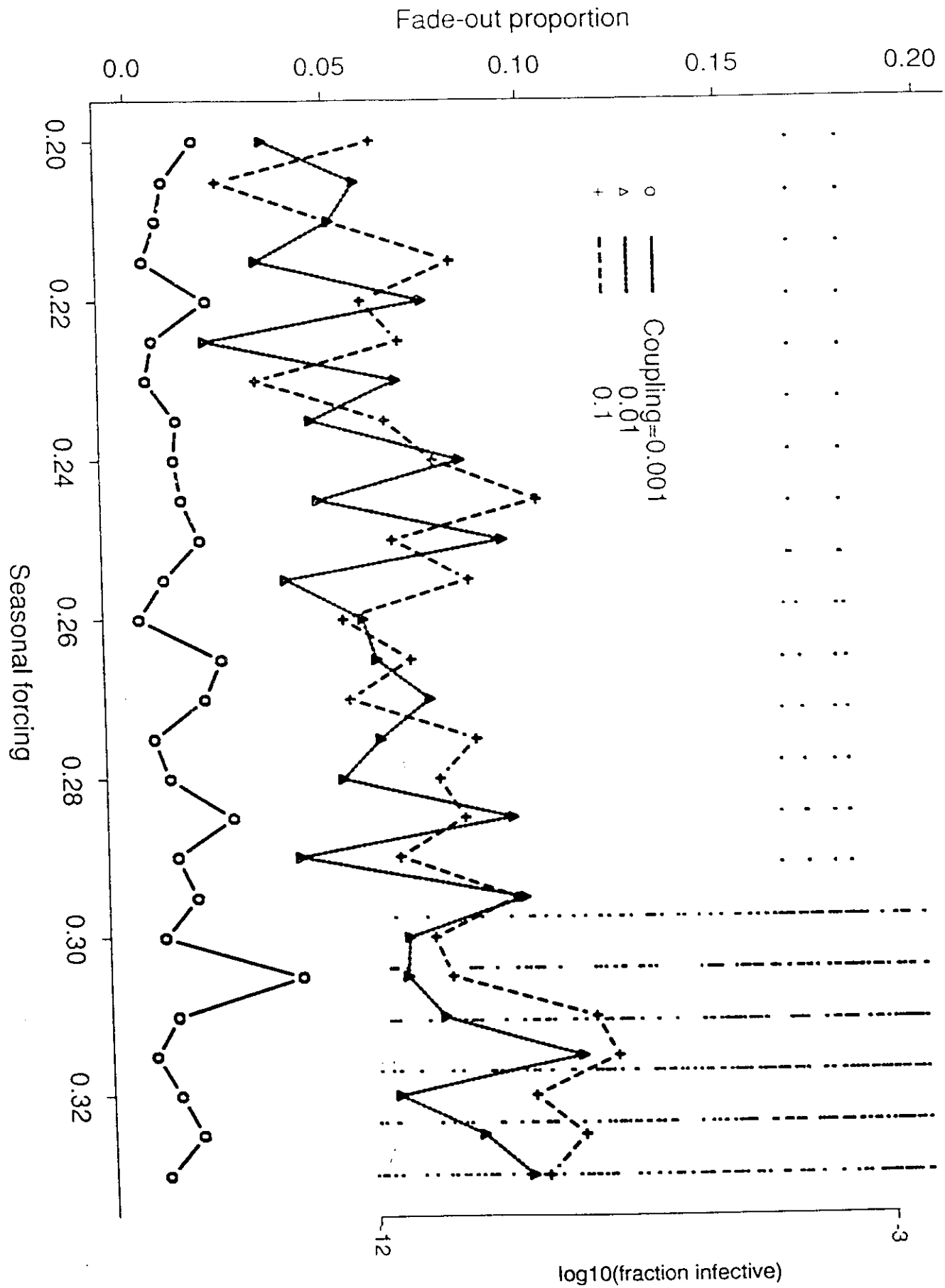
Fade-out proportion
0.0
0.05
0.10
0.15
0.20
Seasonal forcing
0.20
0.22
0.24
0.26
0.28
0.30
0.32
Coupling=0.001
0.01
0.1
log10(fraction infective)
-12
-3

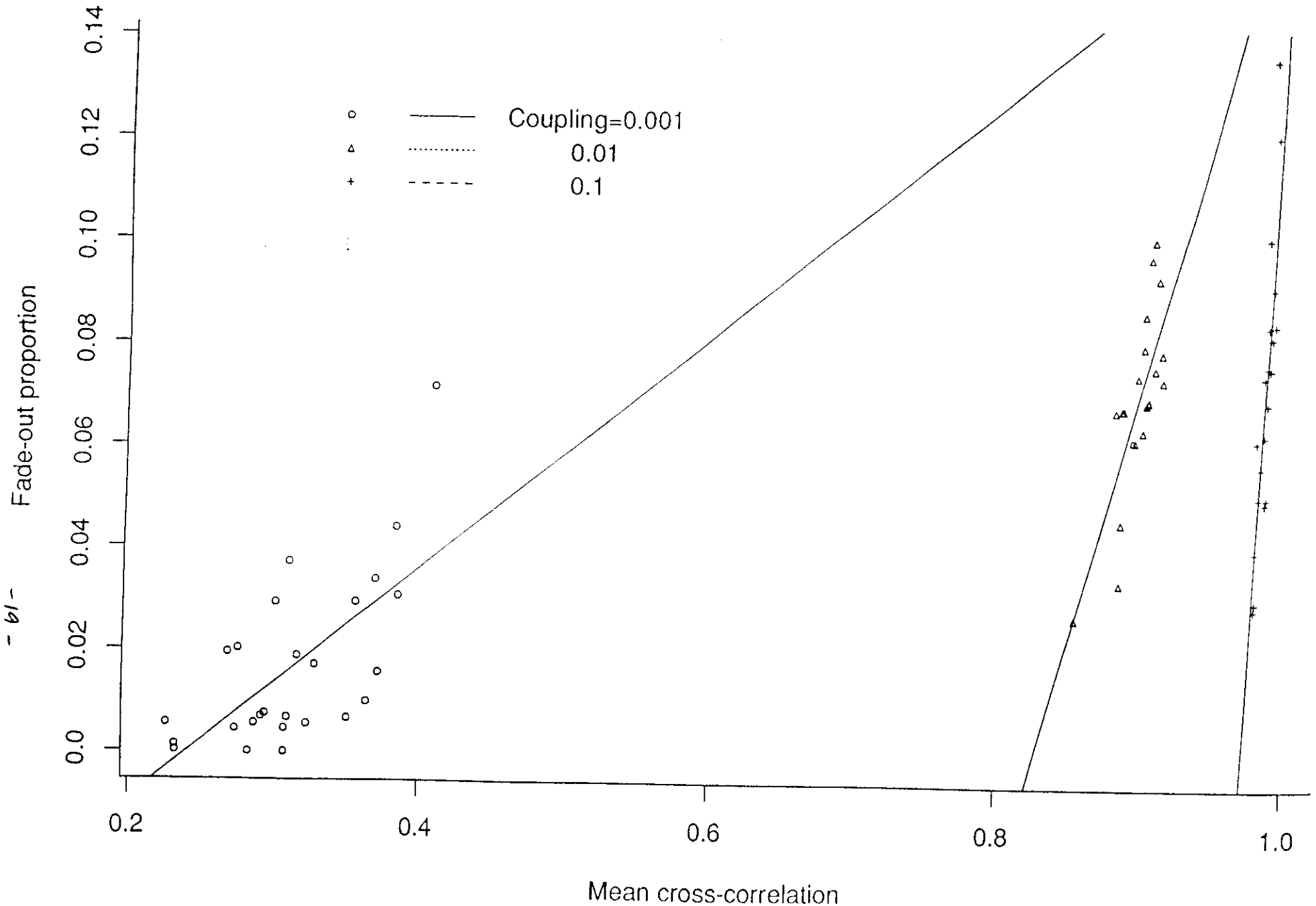
Coupling=0.001
0.01
0.1
Fade-out proportion
0.0
0.02
0.04
0.06
0.08
0.10
0.12
0.14
0.2
0.4
0.6
0.8
1.0
Mean cross-correlation

Fig 3

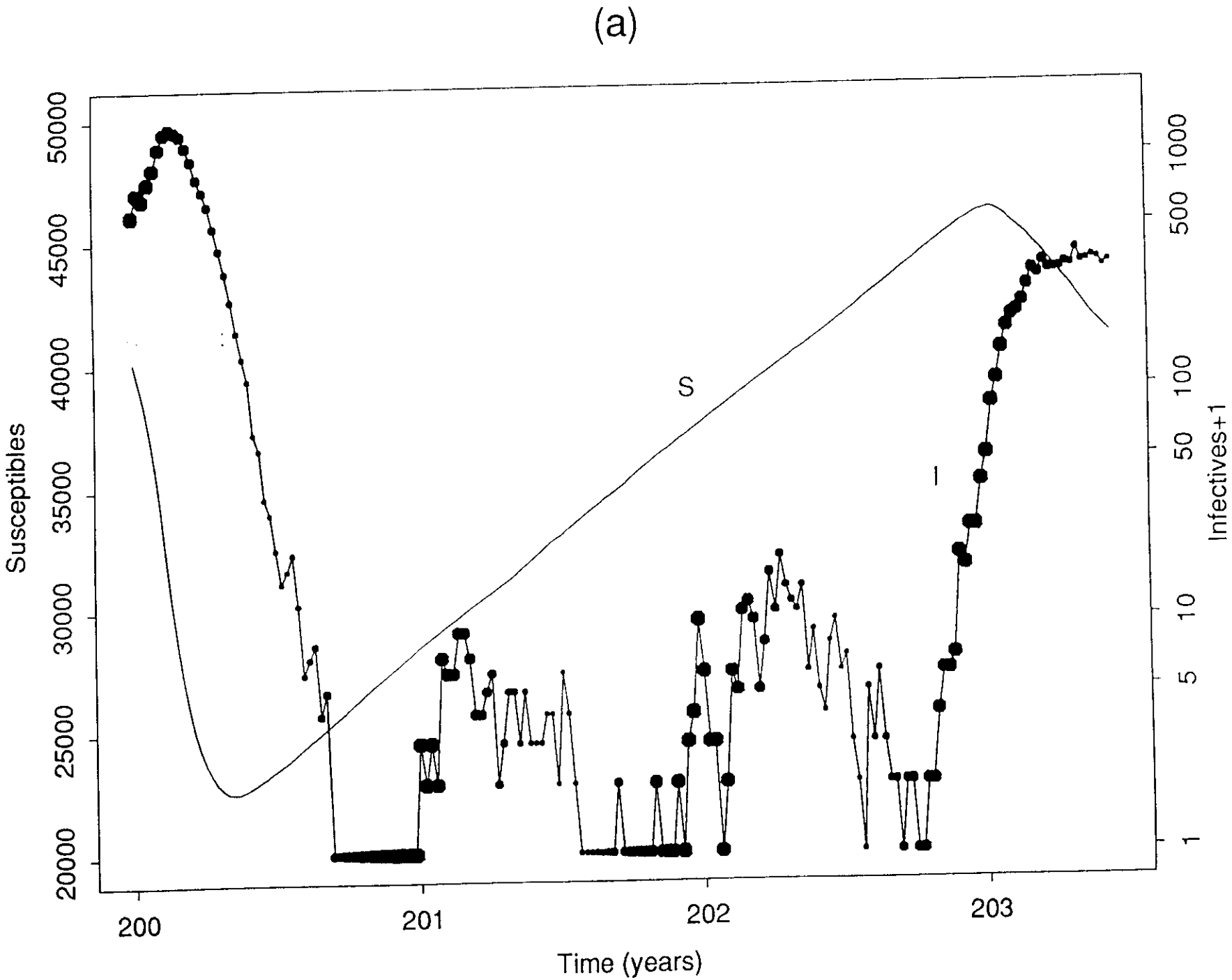
(a)
Susceptibles
Infectives+1
Time (years)
S
I
20000
25000
30000
35000
40000
45000
50000
1
5
10
50
100
500
1000
200
201
202
203

Fig 3

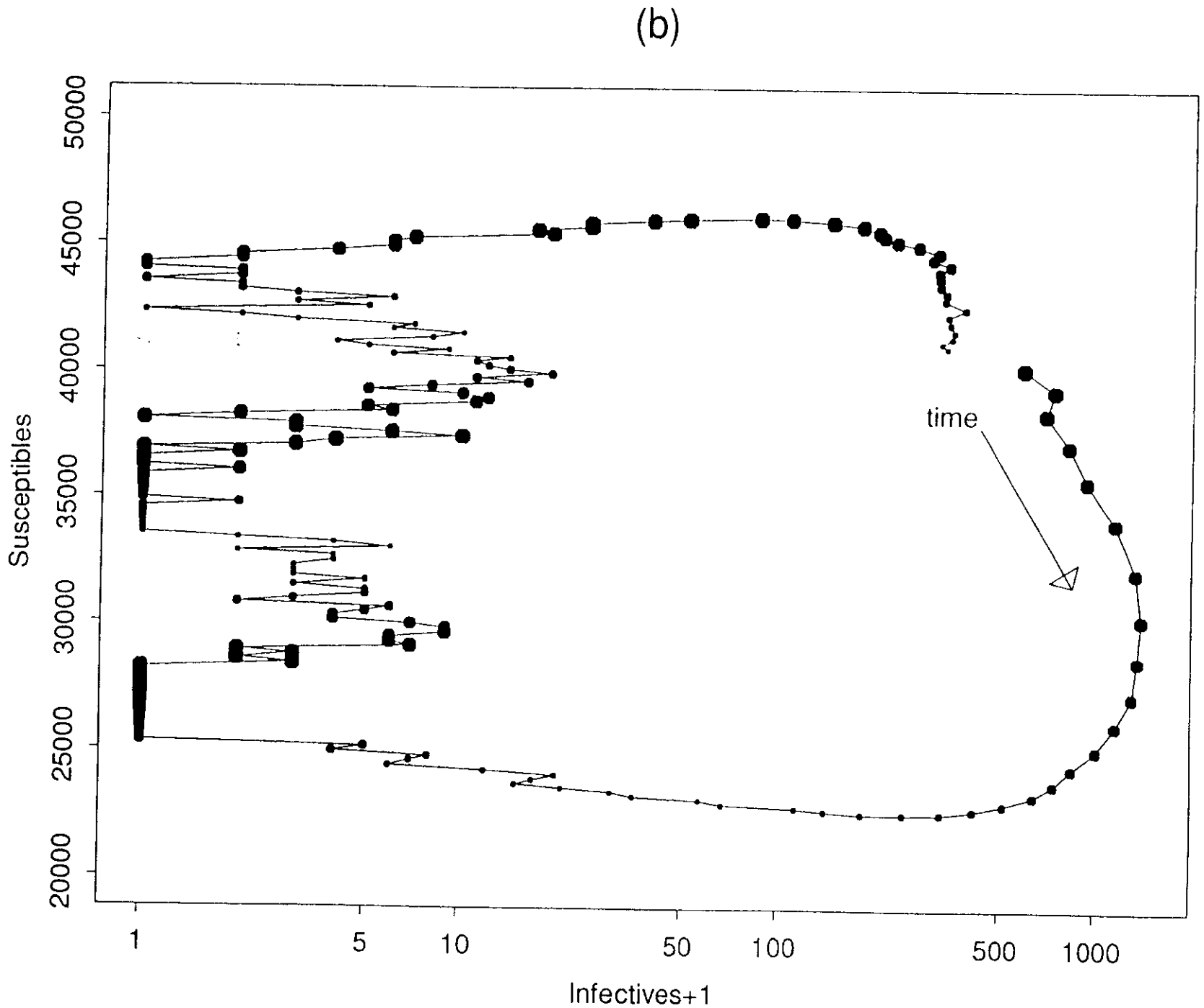
(b)
Susceptibles
50000
45000
40000
35000
30000
25000
20000
time
1
5
10
50
100
500
1000
Infectives+1

Fig 5

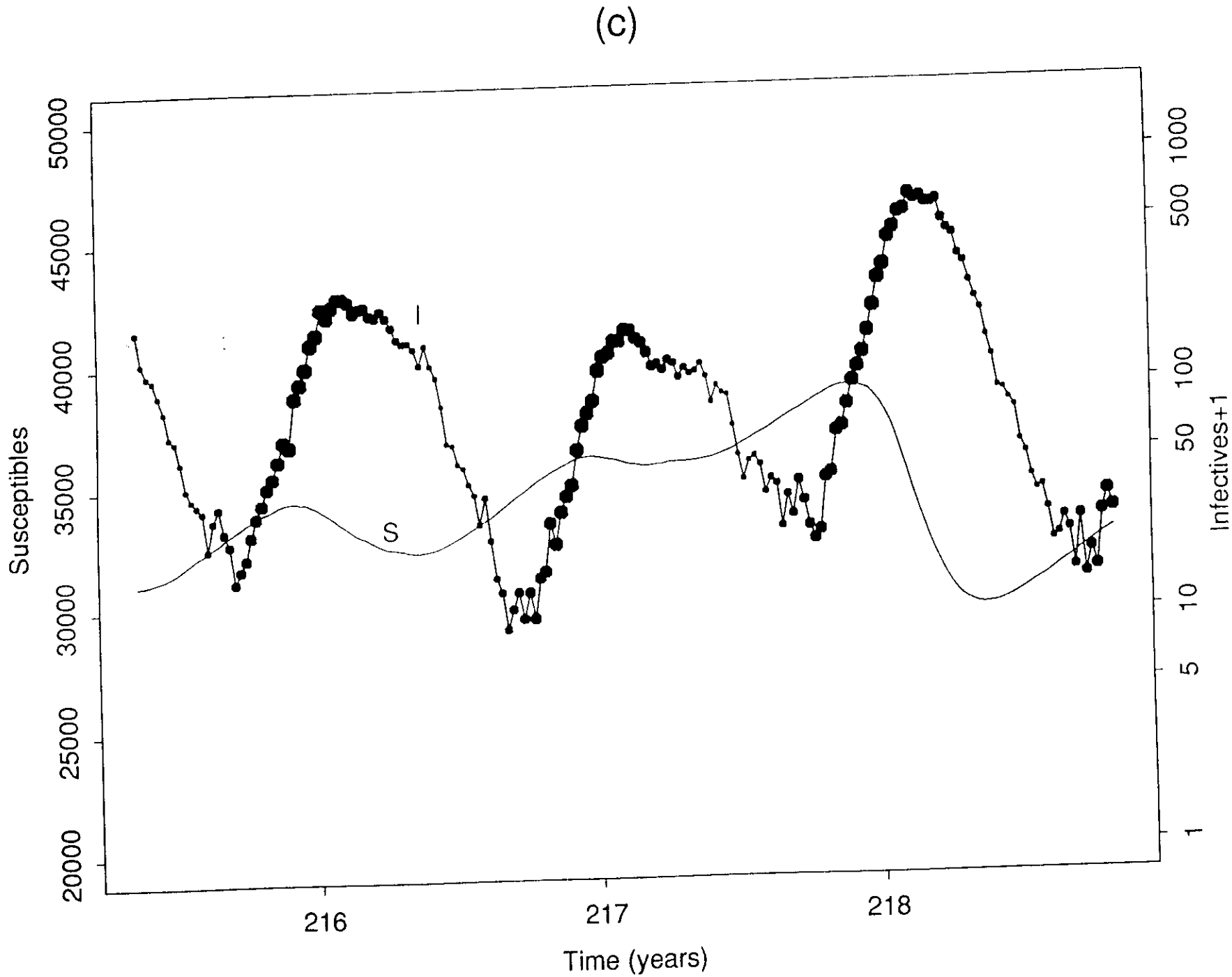
(c)
Susceptibles
20000
25000
30000
35000
40000
45000
50000
Infectives+1
1
5
10
50
100
500
1000
I
S
216
217
218
Time (years)

Fig 3

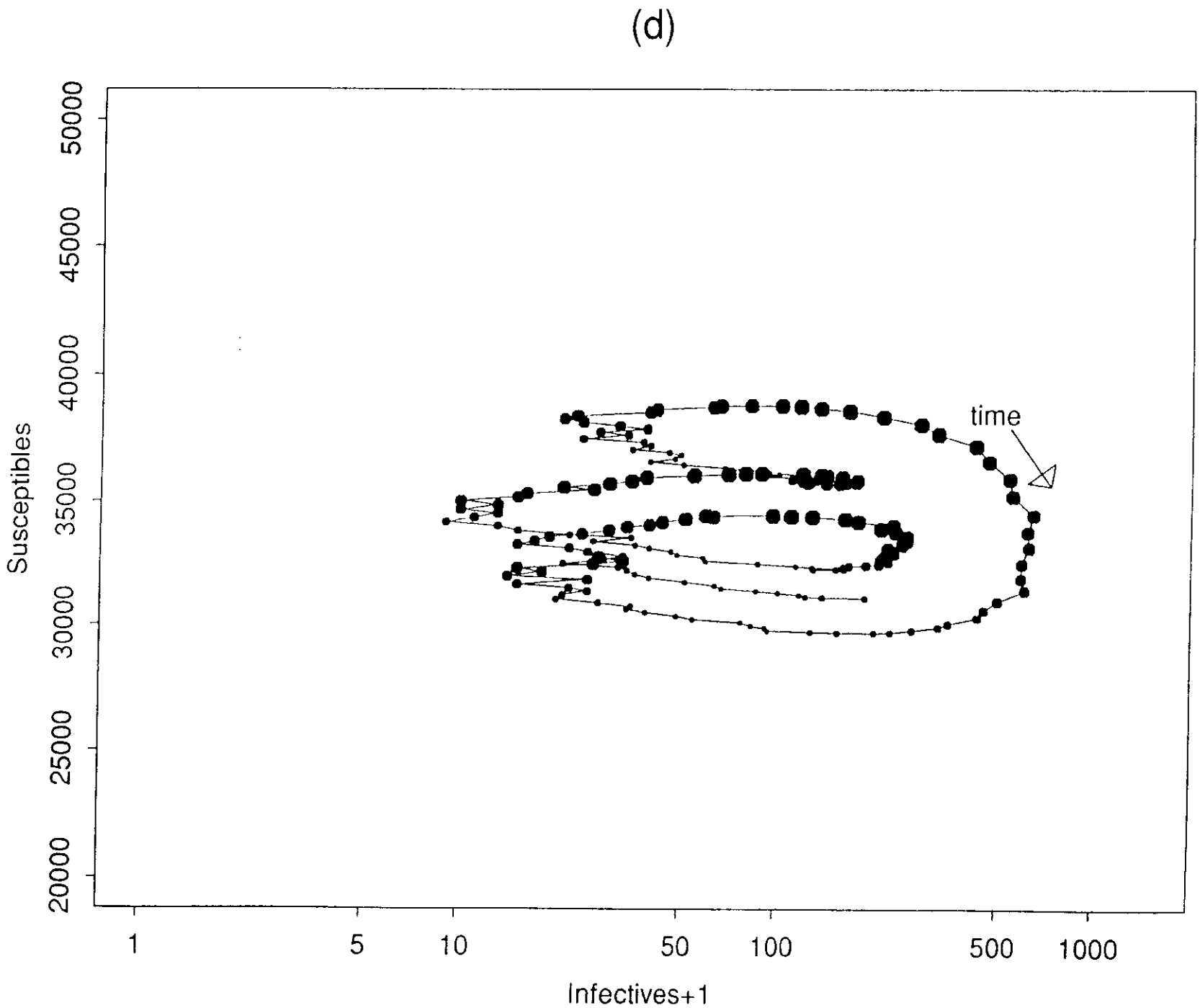
(d)
Susceptibles
20000
25000
30000
35000
40000
45000
50000
time
1
5
10
50
100
500
1000
Infectives+1

Fig 4

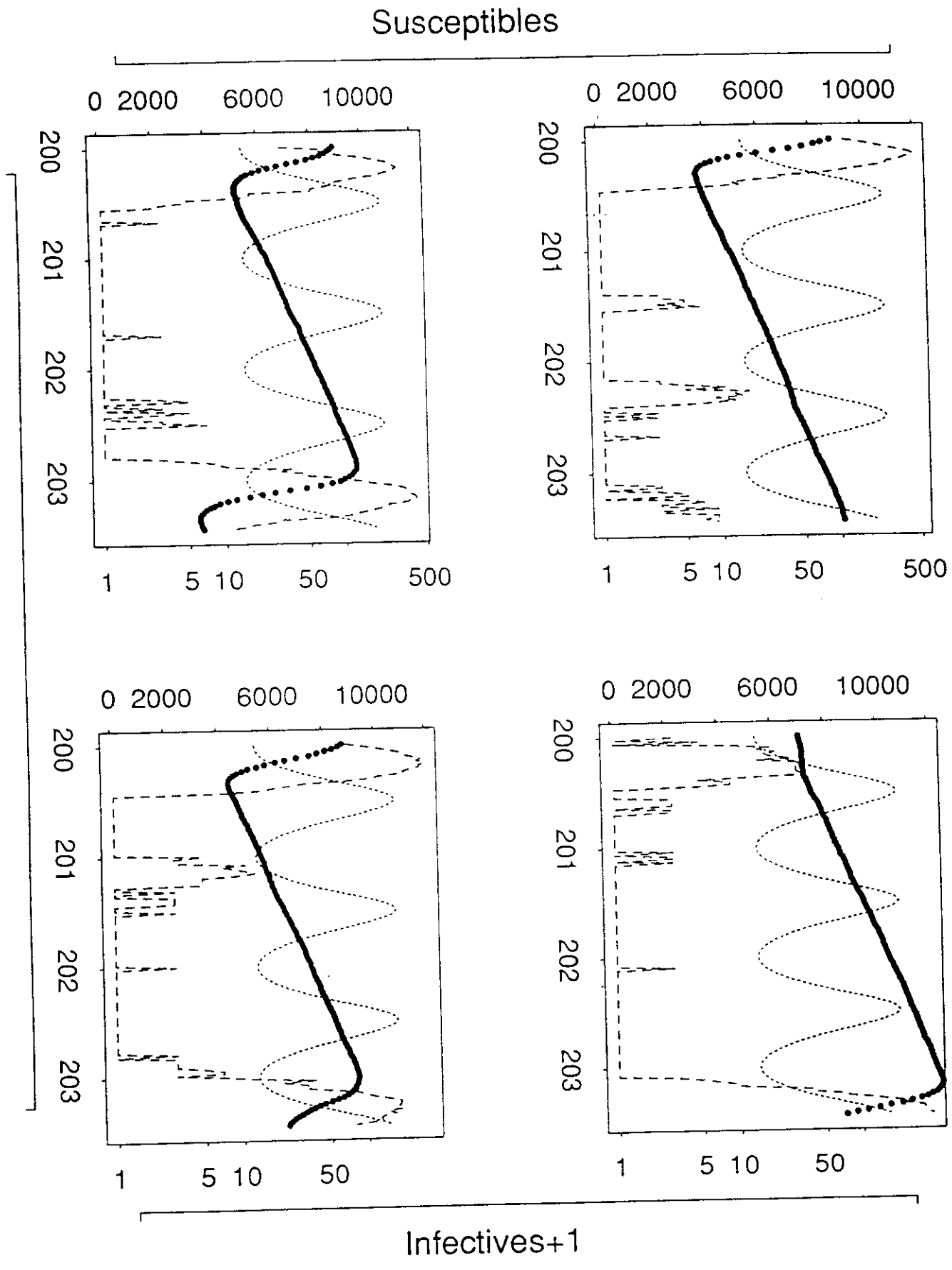
Susceptibles
0 2000 6000 10000
200
201
202
203
1 5 10 50 500
Time
Infectives+1

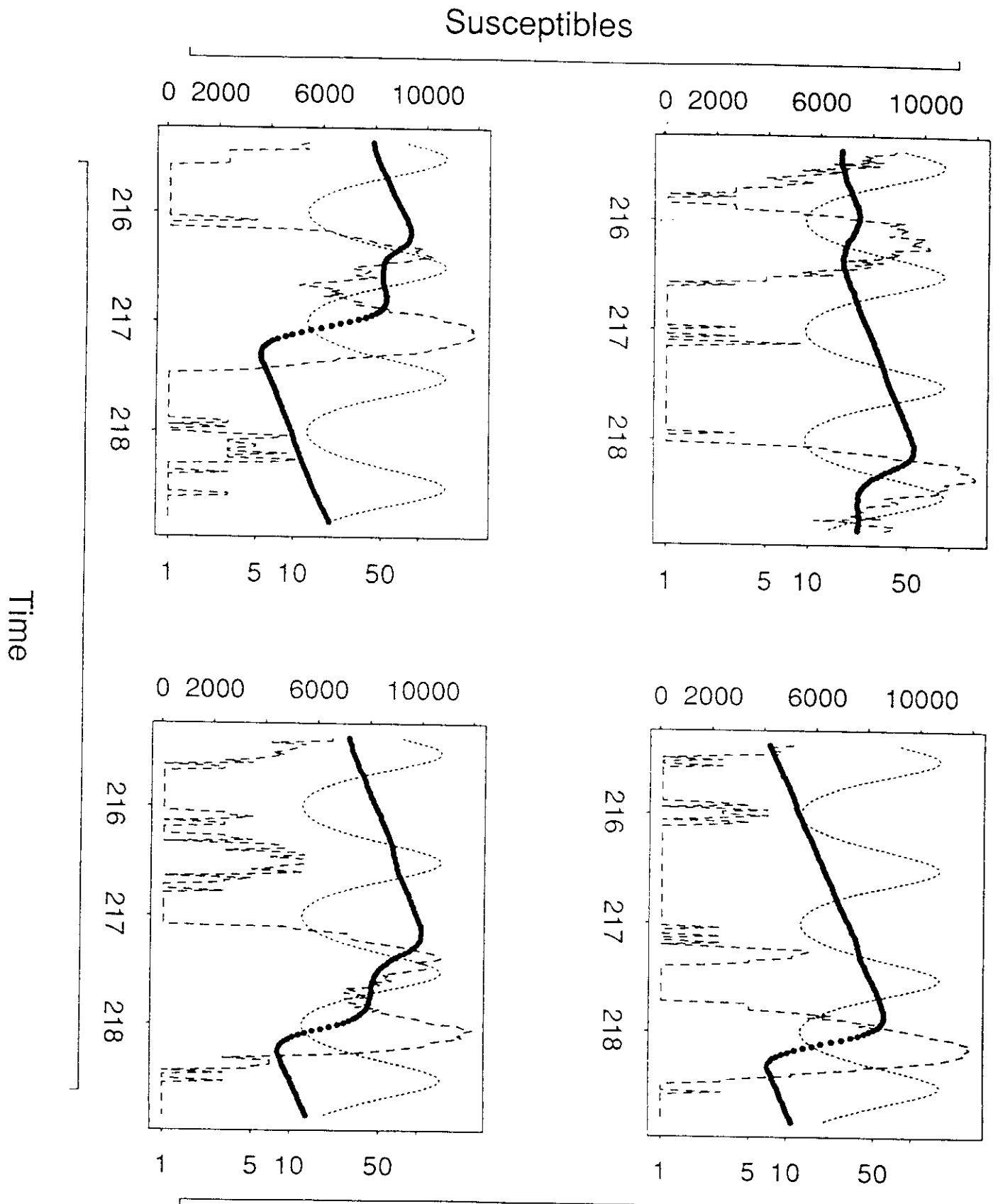
Susceptibles
0 2000 6000 10000
216
217
218
1 5 10 50
Time
Infectives+1